AN ANALOG VLSI COCHLEA WITH NEW TRANSCONDUCTANCE AMPLIFIERS AND NONLINEAR GAIN CONTROL

Rahul Sarpeshkar[1] *Richard F Lyon*[2] *Carver A Mead*[1]

[1]Physics of Computation Laboratory, California Institute of Technology, Pasadena, CA 91125, USA
rahul@pcmp.caltech.edu
[2]Apple Computer, One Infinite Loop, Cupertino, CA 95014, USA
lyon@apple.com

ABSTRACT

We show data from a working 45-stage analog VLSI cochlea, built on a 2.2mm x 2.2mm tiny chip. The novel architectural features in this cochlea are: **1.** The use of a wide-linear-range low-noise subthreshold transconductance amplifier, **2.** The use of "fuse-like" nonlinear positive-feedback amplification in the second-order cochlear filter. Several new circuit techniques used in the design are described here. The fuse nonlinearity shuts off the positive-feedback amplification at large signal levels instead of merely saturating it, like in prior designs, and leads to increased adaptation and improved large-signal stability in the filter. The fuse filter implements a functional model of gain control due to outer hair cells in the biological cochlea. We present data for travelling-wave patterns in our silicon cochlea that reproduce linear and nonlinear effects in the biological cochlea.

1. INTRODUCTION

The electronic cochlea is a cascade of second-order filter sections with exponentially increasing time constants [1]. The design of the second-order filters has evolved to the new topology shown in Figure 1, though the idea of the cochlear cascade remains virtually unchanged. There are four significant changes in the design of the second-order filters, as compared with those in the original cochlea.

1. The transconductance amplifiers marked WLR are now wide-linear-range subthreshold transconductance amplifiers with a linear range of 1–1.5 V or more, instead of amplifiers with a linear range of 75 mV.
2. Since the well is used as an input and as a capacitor in the amplifiers, there are no explicit capacitors in the filters. Thus the capacitors are drawn with dotted lines in Figure 1. Though one might expect that the depletion capacitance of the well would be fairly nonlinear, the well-to-bulk reverse bias is on the order of 3V, the capacitance is fairly constant, and no significant distortion is observed.
3. The positive feedback is now non-monotonic and has a fuse-like characteristic as drawn in the figure, instead of the usual tanh-like characteristic.
4. The positive-feedback amplifier has its output in common with that of the first feedforward amplifier, and has the same differential inputs as that of the second feedforward amplifier. Thus, if its mirror is shared with that of the first feedforward amplifier, and its differential pair is shared with that of the second feedforward amplifier, it need never be completely implemented, and is drawn with dotted lines in Figure 1. The mirror and differential-pair sharing enable the positive-feedback amplifier to be implemented with only four transistors.

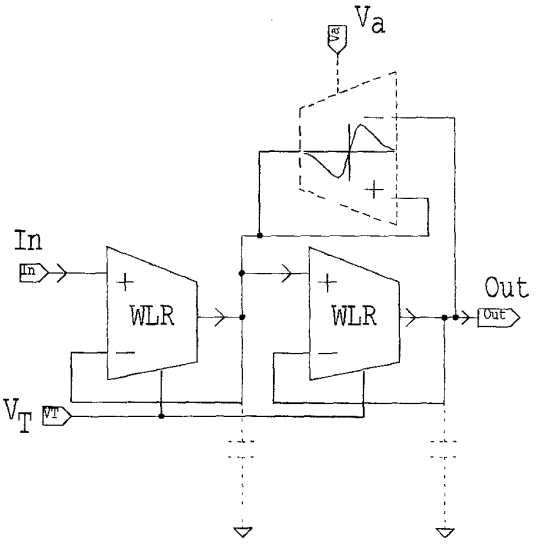

Figure 1. A schematic block diagram of the fuse second-order filter is shown. The dotted lines in the figure indicate that the blocks are not explicitly implemented in the actual circuit of Figure 4. The voltage V_T sets the bias current/corner frequency of the filter. The voltage V_a sets its 'Q' or resonant gain.

2. THE WIDE-LINEAR-RANGE TRANSCONDUCTANCE AMPLIFIER

Figure 2 shows the circuit of the wide-linear-range amplifier. Some details of its operation are described in [2]. The wide linear range is achieved by reducing the transconductance with a combination of four techniques:

0-7803-3073-0/96/$5.00 ©1996 IEEE

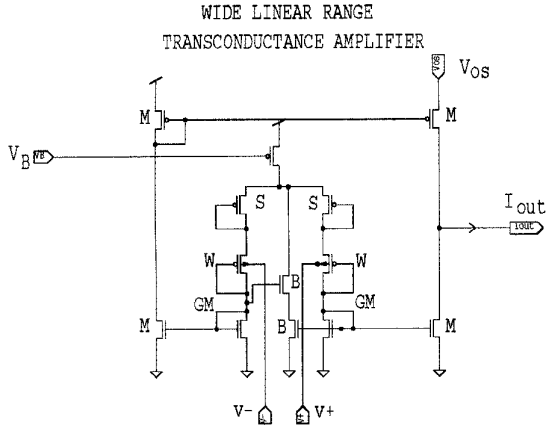

Figure 2. The circuit diagram for the wide-linear range transconductance amplifier is shown. The voltage V_B sets the bias current of the amplifier. The voltage V_{os} allows a fine adjustment of its offset if necessary.

1. The well is used as an input since it has lower transconductance than the gate. The transistors marked W in Figure 2 have their well terminals used as inputs. The topology of the amplifier guarantees that the well-source junction will not be forward biased so long as the input d.c. voltage lies in the 1V–5V range. When the junction is forward biased, the amplifier's bias current simply gets shunted to ground by the parasitic bipolar transistors that turn on. Since subthreshold bias currents are very small, there is no danger of latchup. We have almost never observed latchup even in very complex chips.

2. The transistors marked S in Figure 2 have the transconductance of the W transistors further reduced through the usual technique of source degeneration.

3. The transistors marked GM in Figure 2 reduce the transconductance of the W transistors further through the use of a new technique that we call **gate degeneration**. The idea is simply that increases in current in either arm cause an increase in voltage on the GM diode-connected transistor; the increase in voltage is fed back to the gate of the GM transistor and turns it off. Thus, the degeneration or weakening of the gate reduces transconductance in the same manner as the degeneration or weakening of the source reduces transconductance.

   If κ, κ_n, and κ_p are the exponential subthreshold coefficients of the W, GM and S transistors respectively, then the transfer function of the overall amplifier *with the B transistors absent* is described by the following equations,

$$I_{out} = I_B \tanh(V_d/V_L) \quad (1)$$

$$V_d = V_+ - V_- \quad (2)$$

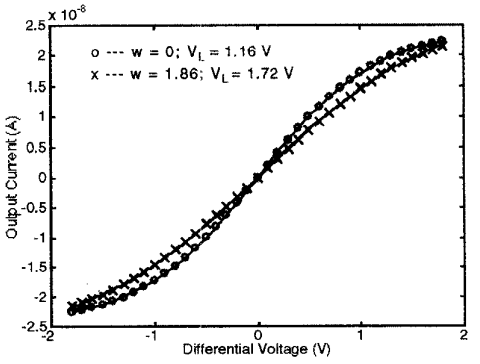

Figure 3. I-V curves for the transconductance amplifier with and without the B transistors are shown.

$$V_L = (2kT/q)\left(\frac{1 + 1/\kappa_p + \kappa/\kappa_n}{1 - \kappa}\right) \quad (3)$$

where I_B is the bias current of the amplifier, and kT/q is the thermal voltage. The $1 - \kappa$ term is due to the use of the well as an input, the $1/\kappa_p$ term is due to source degeneration, and the κ/κ_n term is due to gate degeneration.

4. The transistors marked B steal current from the arms of the differential pair at low differential voltages, and reduce transconductance. At large differential voltages, they are ineffective. It may be shown that if the W/L of the B transistors is w, and that of all other transistors is 1, then, the transfer function of the overall amplifier has the form

$$I_{out} = I_B \frac{\sinh(2x)}{1 + w/2 + \cosh(2x)} \quad (4)$$

where $x = V_d/V_L$.

At $w = 2$, the Taylor series expansion of eq. (4) has no cubic term and only a linear and fifth-order term. Thus, third harmonic distortion is minimized as compared with a tanh-like characteristic. In fact for $w = 2$, eq. (4) yields $I_{out} = I_B(2x/3)$ for small x. Thus, for small x, the addition of the B transistors acts effectively like $V_L \rightarrow (3/2)V_L$ in eq. (1). Empirically, we find that this prescription works for large x as well, and eq. (1) is a good fit to eq. (4), if a larger value of V_L is used. In other words, the B transistors effectively widen the linear range by a factor of 3/2. Figure 3 shows experimental data that yields $V_L = 1.12$ V without the B transistors, and $V_L = 1.72$ V with the B transistors; the ratio of these numbers is near 1.5. An exact fit to eq. (4) showed that w was 1.86 rather than 2. The characteristic of the overall amplifier is robust to larger offsets in w of even 50–100%.

Theory and measurements of noise in a follower-integrator built with a transconductance amplifier and capacitor show that the net rms noise voltage v_n is mostly due to thermal

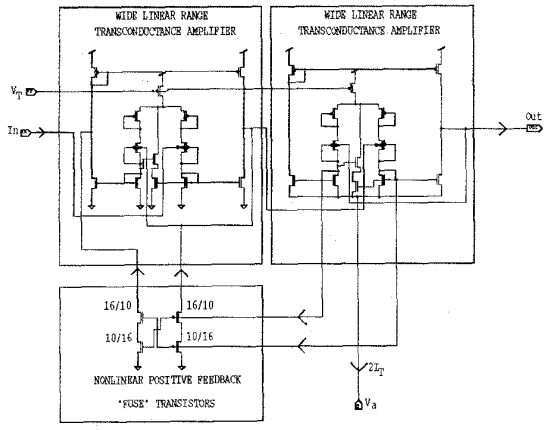

Figure 4. The fuse second-order filter circuit is shown. The details of the circuit are described in the text.

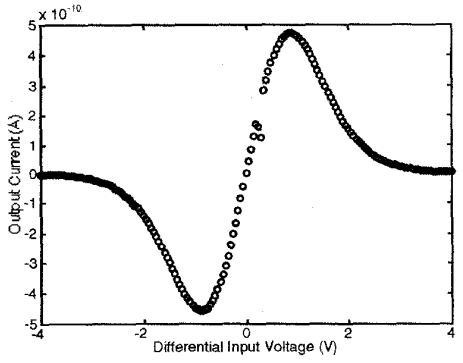

Figure 5. The non-monotonic characteristics of a fuse amplifier built with $w_2 = 16/10$, and $w_1 = 10/16$ are shown.

noise, and is described by

$$v_n^2 = NqV_L/C \tag{5}$$

where q is the charge on the electron, N is the effective number of devices contributing noise in our amplifier, V_L is the linear range of the amplifier, and C is the value of the capacitor (for a discussion of noise in subthreshold devices, see [3]). Though N could potentially be as large as 12 in our circuit, there is noise reduction due to differential cancellation of current noise sources from both arms of the circuit, and due to the shunting of these sources by low conductance pathways; thus N is reduced to be somewhere between 5 and 6. The largest input signal that we can put into the follower-integrator without obtaining too much harmonic distortion is limited by the linear range V_L. Experimentally, for $C = 1$pF, we obtain an rms noise voltage of 0.5–1.0 mV, and total harmonic distortion of less than a percent around an input voltage of 1V rms. Thus,

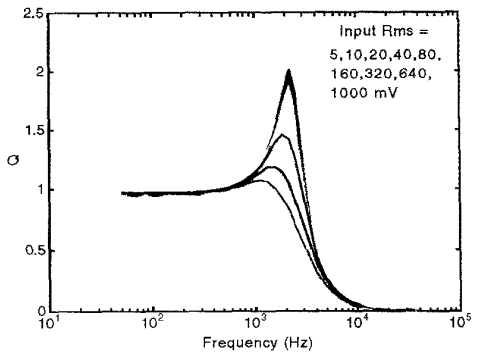

Figure 6. Experimental data illustrating the nonlinear gain-control of the fuse second-order filter are shown. The sharply-peaked high-gain curves correspond to low input amplitudes and the broad low-gain curves correspond to high input amplitudes.

the dynamic range is more than 60 dB. Our design is an order-of-magnitude improvement over early designs [1] that had a dynamic range of 20–40 dB at best.

3. THE FUSE SECOND-ORDER FILTER

The sharing of mirrors and differential pairs in the second-order filter topology of Figure 1, and the use of the amplifier of Figure 2, results in the circuit Figure 4. The nonlinear positive feedback consists of four fuse transistors with W/L's of $w_2 = 16/10$ and $w_1 = 10/16$ in series configuration as shown. They output a current proportional to a nonlinear function of the second amplifier's differential-arm currents, into the first amplifier's output. The positive arm of the fuse shares the mirror of the first amplifier in order to output the correct sign of current. The voltage V_T sets the bias current of the amplifiers and thus the corner frequency of the filter. The voltage V_a modulates the overall positive-feedback current and thus regulates the Q.

For any differential voltage across the second amplifier's terminals, there will be a corresponding differential voltage on the gates of the GM transistors (see Figure 2). The voltages on the gates of the GM transistors are inputs to the gates of the fuse transistors in each arm. Since the current in each series-connected fuse arm is limited by the smaller of its input voltages, its output current is a bump-like function of the input differential voltage. The asymmetry in W/L's moves the peak of the bump away from the origin; the greater the asymmetry w_2/w_1, the further is the peak from the origin. The positive fuse arm has its peak to the right of the origin and the negative fuse arm has its peak to the left of the origin. Thus, the difference between the currents in each arm yields the overall fuse characteristic shown in Figure 5. The data of the figure were obtained from a separate test fuse amplifier on another chip. Figure 6 shows the nonlinear characteristics of a fuse second-order filter. We clearly see the distinct adaptation in Q, with a slight adaptation in corner frequency for various rms input amplitudes. The smallest input amplitudes have the highest Q's

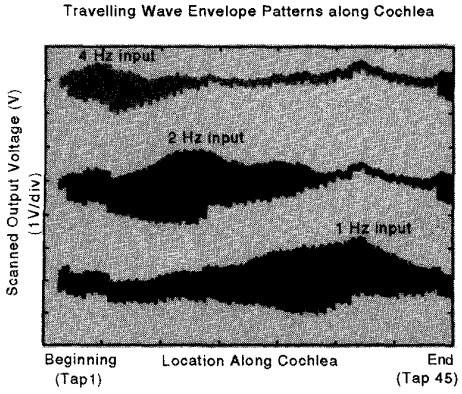

Figure 7. The frequency-to-place encoding of the cochlea is revealed in the shift of the travelling-wave pattern from the end (low-frequency filters) to the beginning (high-frequency filters) as the input frequency is increased.

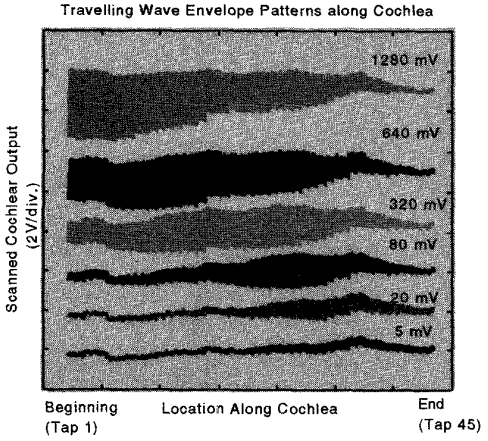

Figure 8. Several nonlinear effects present in the silicon cochlea mimic those seen in the biological cochlea. See Section 4 for an explanation.

and the largest input amplitudes have the lowest Q's. The adaptation occurs mostly after the input rms amplitude is over 160 mV. We picked a w_2/w_1 ratio of approximately $(16/10)^2$ since this choice yielded low harmonic distortion at the output of the second-order filter.

In prior cochlear designs, the large-signal stability limit of the second-order filter was less than its small-signal stability limit [1]. This unfortunate circumstance resulted in the gain at small-signal levels being conservatively small in order that the filter remain stable at large-signal levels. A solution to the problem required having a separate differential amplifier with a small linear range for the positive-feedback amplifier. The fuse filter is large-signal stable even if there are small-signal instabilities because the positive feedback is shut off quickly. It avoids the need for separate differential amplifiers that add more circuitry, noise and offset to the cochlea. Further, the amount of adaptation is controllable, unlike in prior designs; the adaptation may be decreased/increased by raising/lowering the ratio w_2/w_1. The fuse filter is an abstract functional model of the gain control performed by the nonlinearity of outer hair cells in the real biological cochlea.

4. COCHLEAR RESPONSES

Figure 7 shows the envelopes of travelling-wave patterns of the cochlea for a 200 mV rms sinusoidal input at various frequencies. The frequencies over which the cochlea was tuned were purposely made low so that we could see the travelling-wave properties of the cochlea on an oscilloscope. The patterns were obtained by scanning the cochlear analog output waveforms. Figure 8 shows the envelope of travelling-wave patterns of the cochlea for a 2-Hz input and various input rms values. Four effects seen in the biological cochlea are also seen in the silicon cochlea:

1. The frequency-to-place encoding is seen in Figure 7.
2. The shift in the peak of excitation to the beginning of the cochlea at higher input amplitudes is seen in Figure 8. In the biological cochlea, these shifts are almost entirely due to changes in Q. In the silicon cochlea, they are mainly due to changes in Q and secondarily due to changes in corner frequency.
3. The broadening of the pattern of excitation due to the increase in bandwidth of the filters at high input levels (lowering of Q) is seen in Figure 8.
4. Figure 8 shows that even with large changes in the input rms amplitude, there is little change in output rms amplitude at the center or three-quarter's point of the cochlea; small-amplitude inputs are amplified and large-amplitude inputs are attenuated, so that all input amplitudes reach similar output amplitudes. The compression of input rms amplitude is a consequence of the fact that the net adaptation of a cascade of fuse filters is enormous, even though each filter only adapts its Q a little. Thus we illustrate that the accumulative effects of small gain changes in the outer hair cells of the cochlea can result in large amounts of compression and wide input dynamic range.

Acknowledgements

This work is supported by The Beckman Hearing Center.

REFERENCES

[1] C. A. Mead, *Analog VLSI and Neural Systems*, pp. 179–192, and pp. 279–302, Addison Wesley, Reading, MA 1989.

[2] R. Sarpeshkar and C.A. Mead, "CMOS Low-Power, Wide-Linear-Range, Well-Input, Differential and Transconductance Amplifiers", U.S. Patent Ser. No. 5,463,348, Oct. 31, 1995.

[3] R. Sarpeshkar, T. Delbrück, and C.A. Mead, "White Noise in MOS Transistors and Resistors", *IEEE Circuits and Devices*, vol. 9, no. 6, pp. 23-29, Nov. 1993.

AN ANALOG VLSI COCHLEA WITH NEW TRANSCONDUCTANCE AMPLIFIERS AND NONLINEAR GAIN CONTROL

Rahul Sarpeshkar[1] , *Richard F Lyon*[2] *and Carver A Mead*[1]

[1]Physics of Computation Laboratory, California Institute of Technology, Pasadena, CA 91125, USA

rahul@pcmp.caltech.edu

[2]Apple Computer, One Infinite Loop, Cupertino, CA 95014, USA

lyon@apple.com

We show data from a working 45-stage analog VLSI cochlea, built on a 2.2mm x 2.2mm tiny chip. The novel architectural features in this cochlea are: **1.** The use of a wide-linear-range low-noise subthreshold transconductance amplifier, **2.** The use of "fuse-like" nonlinear positive-feedback amplification in the second-order cochlear filter. Several new circuit techniques used in the design are described here. The fuse nonlinearity shuts off the positive-feedback amplification at large signal levels instead of merely saturating it, like in prior designs, and leads to increased adaptation and improved large-signal stability in the filter. The fuse filter implements a functional model of gain control due to outer hair cells in the biological cochlea. We present data for travelling-wave patterns in our silicon cochlea that reproduce linear and nonlinear effects in the biological cochlea.